Tracking Leukocytes *in vivo*

Ahmed S. Mahdi, A M. Artoli , Hassan I. Mathkour

Department of Computer Science, College for Computer and Information Sciences
King Saud University, 11543, KSA

Abstract—Leukocyte tracking invivo is a state of the techniques used for understanding the complex nature of leukocyte recruitment and the transmigration through endothelial cells. It known that the governing force acting on the individual cells are mainly hydrodynamic, the magnitude and nature of the force is not precisely known. This work was a novel segmentation algorithms based on fuzzy logic to track a group of recruited leukocytes captured from video images obtained from invivo experiment on a rat venule. We have found that the force acting on the leukocyte is 0.013998746 dynes under the given experimental conditions.

Keywords- leukocytes, invivo, hydrodynamic, governing.

I. INTRODUCTION

The subject of digital image processing is one of the most important areas which received wide attention and significant progress after the diversified and expanded applications using digital images. It is now one of the most common computer applications to be used in different areas, so not limited to the usual image processing (personal photographic or other), but beyond that to image processing in various fields of science such as: medical image processing[1], production of movies and images[2], remote sensing[3] and control applications[4]. Perhaps the most important in the medical field as x-ray tomography (computed Assisted Tomography) [5], predict cancer in cells where it became possible to diagnose infected cells [6] and discover a human body inflammation using CT image segmentation which have ability to extract pertinent data on via in vivo microscopy[7].

Throughout the inflammation process, our bodies utilize leukocytes to attack infections and assist in repairing destroyed tissue. Nevertheless, in some cases leukocytes can be found when the body incorrectly triggers the inflammatory reaction process, leading leukocytes to attack healthy tissue. These cases can cause a range of problems and diseases, for example joint disease and cardiovascular disease. The motion of leukocytes and their interaction with the endothelium (vessel wall) offers useful details about the inflammation's progression. Automatic tracking algorithms provide the necessary ability to investigate leukocyte movement within living animals.

Many techniques for leukocyte tracking are available. However, in this work, we focused on tracking in vivo microscopy technique. Tracking leukocytes in vivo become increasingly important among medical research groups that are studying inflammatory diseases. Since analysis of leukocyte rolling is an important tool in discovering potential novel anti-inflammatory treatments and in the evaluation of newly discovered drugs [8]. In addition to use in vivo microscopy, a robust and automatic tracking algorithm would also expand the scope of understanding the mechanism of inflammation and involved mediator reactions [9]. For example, E-selectin inhibitors have been shown to reduce the number and increase the velocity of rolling leukocytes in a model of inflammation in living animals [10]. Increased rolling velocity under otherwise identical homodynamic conditions is indicative of weaker, fewer or shorter-lived bonds between the rolling cell and the endothelial lining of the inflamed blood vessel. Currently the analysis of rolling velocities is laborious and requires quite some time of user-interactive image processing work after each experiment. Rolling velocity, stress and vortices are key predictors of inflammatory cell recruitment [11]. In addition to its use in vivo microscopy, a robust and automatic tracking algorithm would also expand the scope of understanding the mechanism of inflammation and involved mediator reactions.

However, acquisition of vivo microscopy image and its processing pose a considerable a challenge for researchers. And the difficulty in image registration in-vivo for living animals based on some reasons such as: physiological activities, safety of a living animal and motion of organs, which makes the process of segmenting and analysis those images very difficult also. As a result of this problem. Analysis, segmentation and tracking leukocytes in capillary will be inefficient and inaccurate. Also, the problem of tracking microscopic moving blood components in venules of less than 30 micrometers is of special interest to our group. The demand for further development in terms of captured video frames made via in vivo microscopy is due to the difficulty in understanding basic biological phenomena related to the mechanism of inflammation, which forces the triggering of autoimmune systems and subsequent activities.

Therefore. In this work, we developed a novel technique to study and analyze the movement and shape of the leukocytes within the capillary on a set of sequential frames of moving blood components within small venules. Images were recorded by in vivo microscopy (commonly known as intravital microscopy) which were previously recorded from a rat experiment in a Lisbon hospital [12], and we then tracked the paths of these cells and automatically calculated the outcome of the forces acting on them under conditions of inflammation. The mathematical model is based on fuzzy logic with log-normal distributions which used to approximate the original histogram [13]. It depends on minimizing the measures of fuzziness. The ranges of

threshold values are sequentially searched to obtain the optimal threshold by performing the proposed procedure. An image must be partitioned into two categories: the foreground whose values are greater than the optimality factor t, and the background whose values are smaller than t. These two categories are modeled as a log- normal distribution. For each pixel in the image, the average of gray levels and membership values are then calculated. Depending on these membership values, the fuzziness of the image is determined using a measure of fuzziness – entropy - which necessitates minimizing the measure of fuzziness of the image effectively in such a way that can be detected by the optimal threshold.

II. RELATED WORK

Tracking leukocytes have gained increasing importance in inflammatory disease studies because the analysis of moving leukocytes is an important process to determine potential novel anti-inflammatory treatments and evaluate newly discovered drugs.

Ray et al. [14] proposed an active contour to track the movement of leukocytes automatically. This approach results in a reduced error in tracking leukocytes, particularly in determining the specific locations of target leukocytes in examination and verification of drugs. Ray et al. [15] further proposed an active contour guided by external forces, in which the direction of hemodynamic flow is considered. These types of techniques depend on the actual intensity gradient of a leukocyte boundary. As cells collide, the boundary between two cells is not evident; thus, the active contour typically fails to segment leukocytes individually. Furthermore, this type of technique is simply used to track individual moving leukocyte at any specific time.

Cui et al. [16] presented a Monte Carlo tracker to automatically track leukocytes in vivo. This tracker depends mainly on leukocyte motion and image intensity. Monte Carlo tracker exhibits higher performance than active contour, and the former is less affected by image noise the latter.

Mukherjee et al. [17] proposed a new method that tracks more than one leukocyte by using image-level sets calculated on the basis of threshold decomposition. This method is appropriate to track leukocytes with slow motion with respect to the frame rate, which is three pixels per frame. Eden et al. [18] designed an automatic technique to extract the rolling velocity of a leukocyte.

Increased rolling velocity under identical homodynamic conditions indicates weak, few, or short-lived bonds between a rolling cell and the endothelial lining of the inflamed blood vessel. Currently, the analysis of rolling velocities is tedious and time consuming, particularly in user-interactive image processing after each experiment. Rolling velocity, stress, and vortices are the key predictors of inflammatory cell recruitment [19]. A robust and automatic tracking algorithm expands the understanding of the mechanism of inflammation and involved mediator reactions in addition to applications in intravital microscopy.

In some cases, a vessel wall is modeled as an isolated protein that supports leukocyte rolling in a planar lipid bilayer or is directly immobilized on glass or plastic. In other cases, this vessel wall is modeled using endothelial cells grown on the lower plate of a flow chamber. Centroid trackers successfully track leukocytes rolling on a transparent substrate, such as protein-coated plastic; however, tracking is difficult when leukocytes are rolled over endothelial cells. This difficulty is due to the structural clutter and obstructions introduced by the optical properties of endothelial cells.

High-throughput approaches have been developed by employing hydrodynamic focusing. In these systems, cells are visualized by phase contrast microscopy, a technique that can yield a "bright" or "dark" image of a cell depending on the position of the focus of the objective with respect to the rolling cell. These techniques and other approaches benefit from a robust tracking algorithm that can track leukocytes even in the presence of clutter, obstruction, and change in focus. Challenging applications involve intravital microscopy, in which rolling cells are observed in living microvessels (in vivo) under inflammation conditions. These experiments add motion artifacts to image processing, and no currently existing algorithm has been successful at tracking rolling leukocytes in vivo [20].

Zhenjiang et al. [21] introduced a particle filter to enhance tracking performance and correctness. Fuzzy logic operations are used to calculate the number of particle filters. An effective and accurate result is obtained when this approach is used to track rolling leukocytes in vivo.

Fuzzy logic was introduced in 1965 by Zadeh [22], who extracted information from fuzzy set theory to present approximate reasoning instead of a precise conclusion from classical predicate logic. Fuzzy logic is a mathematical approach proposed to explain uncertainties. Fuzzy logic has improved applications, particularly image processing, such as edge detection [23-25], image enhancement [26], classification [27], and clustering [28]. Fuzzy logic is a simple and quick method used to obtain a clear conclusion from ambiguous and inaccurate information

This study aimed to develop a method that can be used to calculate the tracks of leukocytes and compute the forces acting on these cells. To the best of our knowledge, force calculations from real in vivo measurements are rarely reported [20].

III. PROPOSED METHOD

The field of digital image processing is one of the most important areas that has attracted great attention and achieved significant progress in recent years. This may be attributed to recent development in imaging techniques and the high demand for imaging in different fields. Perhaps the most important one is the use of sophisticated image modalities in the medical field for the purpose of extracting vital information for research and treatment purposes. However, the acquisition of in vivo microscopic images and their processing pose considerable challenges for researchers. The difficulty in

image registration in living animals is due to a number of factors, including physiological activities, the safety of the living animals and the motion of target subjects. As a result, the analysis and segmentation of a capillary, for example, is not efficient or accurate. In response, in this study we propose some methods based on image processing approaches to accurately threshold of capillary walls and blood components. And using the outcomes to track a group of recruited leukocytes and found the force acting on one leukocyte.

IV. CAPTURING VIDEO FRAMES

Video was recorded by in vivo microscopy which was previously recorded from a rat experiment in a Lisbon hospital [12]. The experiment took place at Lisbon Hospital in Portugal during 2008. The format of in vivo video was in WMV (Windows Media Video), which was readable in the X-Windows environment. The resolution of the obtained video was 640 × 480. The time period of this video was 9.25 minutes, and this video contains 7054 frames in WMF format .

V. IN VIVO VIDEO SPLIT

We were used Matlab to develop algorithm for splitting in vivo video as illustrated in table 0-1.

```
Algorithm of our method:
Detect the path of in vivo video
Read it.
Create the output file
Compute the total number (n) of frame
(i) in in vivo
Set i=1 the first frame in video
 Write the frame i until i=n where i
is equal to max number of frames.
```

Leukocyte video	Leukocytes images after video split
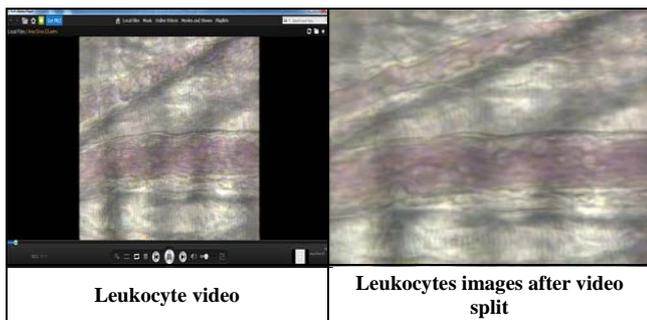
Table 1: Example of leukocyte video splitting

VI. LEUKOCYTES THRESHOLDING

In order to segment the leukocyte from their surroundings (background), an optimal threshold is used to effectively extract the leukocyte from its background. Many algorithms have been developed for this purpose. However, with the development of imaging techniques and the complexity of the product images, there is always a demand for new more robust thresholding algorithms to be proposed.

Fuzzy logic techniques have been used previously for pattern recognition. Most of related work used Gaussian filters to approximate histograms. It is known that the Gaussian filter

is used for symmetric data, which may not be true for most of the captured images. The aim of this work is to explore the state of the art techniques used in thresholding and propose an improvement for the routinely-used Hwang and Wang thresholding techniques. The proposed model is based on fuzzy logic with a log-normal distribution to enable us to deal with asymmetric data. An exclusive review on image thresholding was reported in [29].

Threshold processes give us a binary image with two types of pixels: 0 and 1. The 0 pixel indicates the background (usually stands for the black colour) and the 1 indicates the leukocyte, standing in for the white colour. In many applications of image processing, the grey levels of pixels belonging to the object are quite different from the grey levels of the pixels belonging to the background. Thresholding becomes a simple but effective tool to separate objects from the background. Examples of thresholding applications are document image analysis logos, graphical content, musical scores, map processing, scenes processing, quality inspection of materials, and other applications. Most captured images are associated with noise attributed to a number of physical and non-physical reasons. Noise reduction enhances the signal to noise ratio via a number of different techniques.

VII. MODEL CONSIDERATIONS

We consider a two dimensional digital greyscale image. The image is well represented by a histogram, which gives statistical information about the image's pixels and describes the pixel intensity distribution by graphing the number of pixels at each grey level. Essentially, the two possible shapes (modes) of the grey level distribution are symmetrical and non-symmetrical. For a symmetric mode, the Gaussian distribution works fine for estimating the threshold value. On the other hand, the log-normal distribution is more suitable for a non-symmetrical mode. A log-normal distribution is the probability distribution of a random variable whose logarithm is normally distributed. It has certain similarities to the normal distribution but is positively skewed (skewed to the right). Therefore, the log-normal distribution may be used to model symmetric data or positively skewed data.

$$F(x, \mu, \sigma) = \frac{1}{x.\sigma\sqrt{2\pi}} e^{\frac{1}{2}\left(\frac{\ln x - \mu}{\sigma}\right)^2} \qquad (1)$$

Where μ and σ are the mean and standard deviation of the natural logarithm, respectively, of the random variable and x is the pixel intensity. μ and σ are obtained by:

$$\mu = \log\left(\frac{\hat{m}_1^2}{\hat{m}_2}\right) \quad ; \quad \sigma = \sqrt{\log\left(\frac{\hat{m}_2}{\hat{m}_1^2}\right)}$$

The discrete formulae for these moments are:

$$\mu_{1(t)} = \frac{\sum_{i=0}^{t} h(i) \log(i)}{\sum_{i=0}^{t} h(i)} \qquad \mu_{2(t)} = \frac{\sum_{i=t}^{L-1} h(i) \log(i)}{\sum_{i=t}^{L-1} h(i)}$$

Figure 1 illustrates three shapes of Log-normal distribution with different variable values.
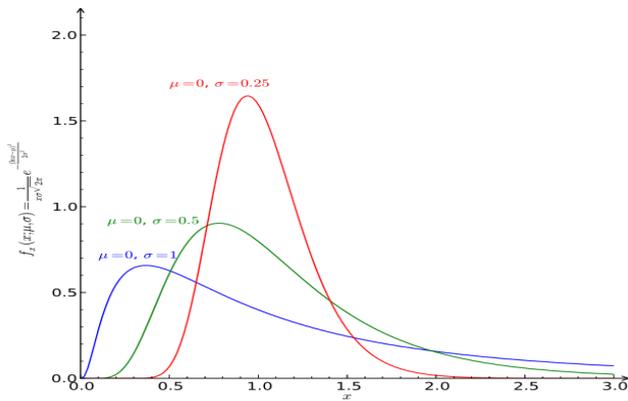
Fig:1 :Log-normal distribution in different cases of σ.

VIII. METHOD

Let I denote a leukocyte image set of size M×N with L grey levels; h (g) denotes the number of occurrences of the grey level g in I. We assume that the data in the image I is modelled by a log-normal distribution. Hence, for a specific threshold value t, the average grey levels in the background and foreground can be obtained from the following equations:

$$\mu_{B,I} = \frac{\sum_{i=0}^{t} h(i)\log(i)}{\sum_{i=1}^{t} h(i)} \qquad (2)$$

Where $\mu_{B,I}$ is the average grey level of background B in image I.

$$\mu_{F,I} = \frac{\sum_{i=t}^{L-1} h(i)\log(i)}{\sum_{i=t}^{L} h(i)} \qquad (2)$$

Where $\mu_{F,I}$ is the average grey level of background F in image I. Let $I_{m,n}$ denote the grey level of the (m, n) pixel in I. The relationship between pixels(m, n) and its belonging region should intuitively depend on the difference of its grey level and the target value of its belonging region. Thus, let the relationship possess the property that the smaller the absolute difference between the grey level of a pixel and its corresponding target, the larger the membership value of the pixel is. Hence, the membership function that evaluates the above relationship for an (m, n) pixel can be defined as:

$$\mu_I\left(X_{I_{m,n}}\right) =$$
$$\begin{cases} \dfrac{1}{1+\frac{\left|X_{I_{m,n}}-\mu_{B,I}\right|}{C}} & X_{I_{m,n}} \leq t \\ \dfrac{1}{1+\frac{\left|X_{I_{m,n}}-\mu_{F,I}\right|}{C}} & X_{I_{m,n}} > t \end{cases} \qquad (3)$$

Here, C is a constant value $\in [0, L]$ such that $0.5 \leq \mu_I\left(X_{I_{m,n}}\right) \leq 1$. The definition of the membership function is intuitive because it should depend on the difference in the grey level $X_{I_{m,n}}$ and the average of its belonging region. In such a way, each of the pixels has its own membership.

Several approaches are proposed for the measurement of fuzziness. Here, we used the entropy measure. The entropy of a fuzzy set is defined using Shannon's function S and

extending the concepts to the two dimensional image planes. Thus, the entropy of image set I is

$$E(I) = \frac{1}{MN} \sum_{g=0}^{L-1} S(\mu_I\left(X_{I_{m,n}}\right) h(g) \qquad (4)$$

Where the Shannon function S is given by

$$S((\mu_I(X_{I_{m,n}})) = -\mu_I(X_{I_{m,n}})\ln\left[\mu_I(X_{I_{m,n}})\right] - \left[1 - (\mu_I(X_{I_{m,n}}))\right]\ln[1 - \mu_I(X_{I_{m,n}})]] \qquad (5)$$

Shannon's function is monotonically increasing in the interval [0, 0.5] and decreasing in the interval [0.5, 1]. When $\mu_I\left(X_{I_{m,n}}\right) = 0.5$, for all m and n, the entropy E will have the maximum measure of fuzziness. Finally, the optimal threshold for the image $t_{Optimal}$ is obtained by computing the entropy measure of fuzziness sequentially for all $t \in [0, L-1]$. The threshold value with the minimum value E(I) is $t_{optimal}$. in the following algorithm of our method:

```
Set t = gi_min, where gi_min, is equal to min
gray level in the original image.
Compute the average of gray levels of
objects and background using equations
(4) and (5).
Calculate the membership function μ_I(X_{I_{m,n}}).
Calculate entropy E(I) and save it.
Go to step 1 until t = gi_max where gi_max is
equal to max gray level in the original
image.
Find Min E(I), ∀ t ∈ [gi_min, gi_max].
The optimum threshold value is t with Min
E(I).
```

The two average grey levels (the two target values) in (4) and (5) are taken as integer values so that the membership value and the measure of fuzziness of each grey level can be evaluated in advance and are stored in a table. When the given threshold value t is iteratively changed from **gi_mim**, to **gi_max** the use of the data in the table can significantly reduce the computation time in Step 2. Hence, it is necessary to construct the table in Step 0. By using the fuzzy range, we can further determine an improved threshold t*, which is the best location of a deep valley in the gray-level histogram. In other words, the threshold t* can be obtained according to the following equation:

Minimize h (g - 1) + h (g) + h (g + 1) (6)

Theoretically, the threshold t* should have a better chance of being located in the real valley than the threshold obtained by minimizing the measure of fuzziness, and it should have a better threshold result in practice. Figure 3:5 shows an example result after the image is thresholded. Optimal values were chosen to give the best identified shape for the leukocytes.

IX. LEUKOCYTE IMAGES

In order to segment the leukocyte from their surrounded (background) was necessary, an optimal threshold is a process used to effectively extract the leukocyte from its background. Now the proposed method will be applied to grayscale leukocytes image which presents as samples on Table :2.

Grayscale Image	Segmented Image
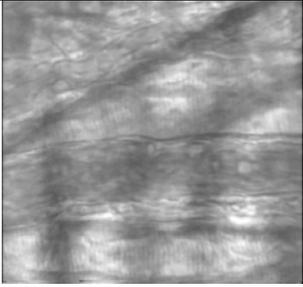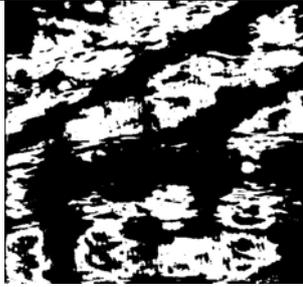
Table VIII2: Segmenting result of leukocytes grayscale images via fuzzy

Original Picture	Fuzzy with Log-Normal
Threshold value	**169**
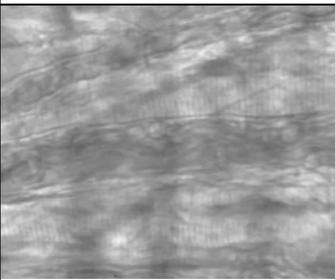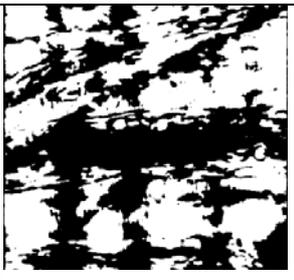
Table 3: Segmenting result of leukocytes grayscale images via fuzzy with log-normal distribution

The optimal threshold of leukocytes image is calculated and used to compare it with the performance of the same method based on the Gaussian distribution. We claim that that fuzzy similarity with log-normal distribution outperforms the Gaussian based Huang and Wang's method

These results show the Gaussian thresholding algorithm based on fuzzy similarity was modified by replacing the Gaussian with the log-normal distribution. This new method solves the problem of dealing with non- symmetric histograms for images. The log-normal method captures both the non-symmetric property .The Huang and Wang's method based on the Gaussian distribution for a range of values of L is tested on various noisy images with large signal to noise ratios. The E(I) is calculated and used to compare it with the performance of the same method based on the Gaussian distribution. We claim that that fuzzy similarity with log-normal distribution outperforms the Gaussian based Huang and Wang's method. However, it should be noted that all of these methods have some drawbacks when dealing with low-contrast images.

The previous result demonstrated that utilization of the Log-Normal distribution outperformance other tested distributions of similar complexity, also Log-Normal edge detector produced continuous and precise edges, and it was also identified edges accurately. The Log-Normal edge detector performs better than all others detectors due to the ability of Log-normal to deal with asymmetric and sympatric data. Beta edge detector identified surprisingly similarly to the Gamma detector, and both have a major drawback of identifying the edges with spotty and not contiguous.

X. FORCES ACTING ON A ROLLING LEUKOCYTE

As shown in Figure 3, the leukocyte has radius R. The blood has a viscosity μ ,density p and approaches the leukocyte vertically upwards along the negative z-axis with uniform velocity v. For very slow flow, the moment flux distribution, pressure distribution and the velocity component in leukocytes coordinate, they have analytically been found to be:

$$\tau_{r\infty} = \frac{3}{2} \frac{\mu v_\infty}{R} \left(\frac{R}{r}\right)^4 \sin\theta \tag{7}$$

$$p = p_0 - \rho gz - \frac{3}{2} \frac{\mu v_\infty}{R} \left(\frac{R}{r}\right)^2 \cos\theta \tag{8}$$

$$v_r = v_\infty \left[1 - \frac{3}{2}\frac{R}{r} + \frac{1}{2}\left(\frac{R}{r}\right)^3\right] \cos\theta \tag{9}$$

$$v_\theta = v_\infty \left[1 - \frac{3}{2}\frac{R}{r} + \frac{1}{2}\left(\frac{R}{r}\right)^3\right] \sin\theta \tag{10}$$

In Equation the quantity p_0 is the pressure in the plane z=0 far away from the leukocyte, ρgz is the contribution of the blood weight (hydrostatic effect), and the term containing v_∞ results from the flow of the blood around the leukocyte.

We note that the velocity distribution satisfies the condition $v_\theta = v_\infty = 0$. At the surface of leukocyte. Furthermore, it may be shown that v_r approaches v_∞ from a distance far from the leukocyte. In addition, the pressure distribution clearly reduces to the hydrostatic equation p=p_0 - ρgz far more the leukocyte surface. Hence the expressions do satisfy the boundary condition that r=R and r= ∞. Let us calculate the net force exerted by the blood on the leukocyte. This force is computed by integrating the normal force and the tangential force over the leukocyte surface [30].

Integration of the normal force shows that at each point on the surface of the leukocyte there is a force per unit area, ρ, on the solid acting perpendicularly to the surface; the z- component of this force is $\rho\cos\theta$. We now multiply this local force per unit area by the surface of the leukocyte to get the resultant force in the z-direction
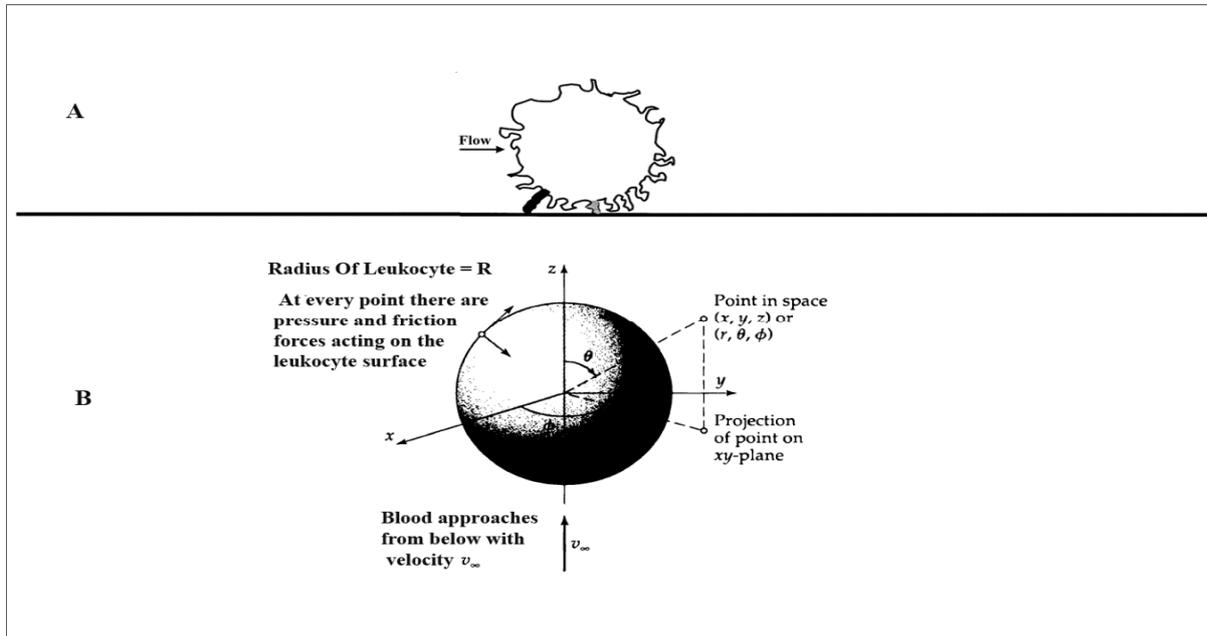
Fig 3: (A) A leukocyte in momentary, static equilibrium during rolling. (B) The coordinate system used in describing the flow of a fluid about leukocyte [30].

$$F_n = \int_0^{2\pi} \int_0^{\pi} (-\rho \setminus r = R^{\cos \theta}) R^2 \sin \theta \, d\theta \, d\phi$$

The pressure distribution on the surface of the leukocyte is

$$\rho \setminus_{r=R} = p_0 - \rho g R \cos\theta - \frac{3}{2} \frac{\mu v_\infty}{R} \cos\theta \qquad (8)$$

We now substitute this expression into the integral in Equation-6. The integral involving p_0 vanishes identically, the integral involving $\rho g R \cos\theta$ gives the buoyant force of the blood on the solid, and the integral involving the velocity gives the "from drag"; hence we ultimately get

$$F_n = \frac{3}{2}\pi R^2 pg + 2\pi\mu R v_\infty \qquad (10)$$

XI. INTEGRATION OF THE TANGENTIAL FORCE

At each point on the surface, there is also a shear stress acting tangentially. This stress $\tau_{r\theta}$ is the face in the θ-direction acting on a unit area of leukocyte surface. The z-component of this force per unit area is ($\tau_{r\theta}$, $\sin\theta$). We now multiply it by $R^2 \sin \theta \, d\theta \, d\varphi$, and integrate it over the leukocyte surface to get the resultant force in the z-direction:

$$F_n = \int_0^{2\pi} \int_0^{\pi} (+r_{r\theta} \setminus r = R^{\sin \theta}) R^2 \sin \theta \, d\theta \, d\varphi \qquad (11)$$

The shear stress direction at the surface of the leukocyte from Equation (1) is

$$\tau_{r\theta} \Big|_{r=R} = \frac{3}{2} \frac{\mu v_\infty}{R} \frac{R}{r} \sin \theta \qquad (12)$$

Substitution of this expression into integral in Equation. 8 the "friction drag"

$$F_n = 4\pi\mu R v_\infty \theta \qquad (13)$$

Hence the total force F of the blood on the leukocyte is given by the sum of Equation. 7 and Equation. 10:

$$F = \underset{\substack{(buoyant \\ force)}}{\frac{3}{2}\pi R^3 pg} + \underset{\substack{from \\ drag}}{2\pi\mu R v_\infty} + \underset{\substack{from \\ frction}}{4\pi\mu R v_\infty} \qquad (14)$$

Or

$$F = \frac{3}{2}\pi R^3 pg + 6\pi\mu R v_\infty \qquad (15)$$

The first term on the right side of the last equation represents the buoyant force and the second result is from the blood motion regarding the leukocyte. It is convenient for later discussions to designate these two terms as F_s (the force exerted, even if the blood is stationary) and F_k (the force associated with the blood movement) [80]. For the problem at hand these forces are:

$$F_s = \frac{3}{2}\pi R^3 pg \qquad (16)$$

$$F_k = 6\pi\mu R v_\infty \qquad (17)$$

XII. TRACK AND FORCE CALCULATION USING PHYSICALLY PROPERTIES

The tracks, velocity and acceleration were smoothed using physically properties and governing force, electromagnetic force and gravitational forces. From theses we were able to compute the average forces. Tracking of leukocytes was made semi-manual due to the restriction resolution of the image and the lack of the available automated segmentation algorithms, owever the aim of this project was to automate the

process of segmentation but not the tracking process. This would a subject of a future work. It was possible to compute the velocity and acceleration for Instantaneous leukocytes.

Thereafter image track is smooth and differentiated trice to obtain the velocity and acceleration and hence the force acting on the leukocytes. We have explained all image operations made on the original image taken from the inverted video frame. Tracks will be differentiated and forces are to be computed according to simple calculus rules. Numerical processing (differentiation) is a candidate on the obtained data. To get the velocity and acceleration. Assuming that the max leukocyte diameter is 15 µm we have calculated the pixel-physical direction relation and have found 1 pixel $\equiv$ 0.6 µm. Now we will track the appearance and disappearance of each leukocyte and we will calculate the time of appearance and disappearance of each leukocyte. According to a specific formula: NFS=total frames/duration of video

$$NFS = \frac{F_t}{t} \qquad (19)$$

Where NFS is number of frames per seconds F_t is the total number of frames in the leukocytes video and to the duration time on video. The total number of frames after deploying the split algorithms equal 7054 and the duration of leukocyte video equal 562 second. So the number of frames per second (NFS) equal 12.48495575 frames per second. As we mention 1 pixel $\equiv$ 0.6 µm, since we must multiply every pixel by 0.6 µm for example.

Table 4: pixel converted to micrometer, F_n the frame number Px_p Position of leukocyte in direction X in pixel, $Px_{\mu m}$ Position of Leukocyte in direction X in micrometers.

Ln	F_n	Px_p	$Px_{\mu m}$
1	1	515	309
2	41	463	277.8
3	65	440	264
4	92	405	243
5	103	403	241.8
6	124	381	228.6
7	146	364	218.4

Table 5: present the appearance and disappearance of 23 leukocytes and its position in Both X and Y-direction and the specific time in appearance and disappearance cases.

L_N	Leukocyte appearance				leukocyte disappearance			
	F_n	p_x	p_y	Time	F_n	p_x	p_y	Time
1	1	309	170.4	0.080096	399	4.8	202.2	31.95846
2	1167	347.4	161.4	93.4725	1499	10.2	153.6	120.0645
3	1459	354	163.8	116.8606	2174	16.2	156.6	174.1296
4	2234	369	178.2	178.9354	2545	42.6	187.2	203.8453
5	2509	67.8	160.2	200.9619	2619	12.6	188.4	209.7725
6	2458	80.4	165	196.8769	2491	97.2	161.4	199.5201
7	2480	376.2	148.2	198.6391	2619	222	154.2	209.7725
8	2790	374.4	142.8	223.469	3193	5.4	194.4	255.7478
9	3473	226.8	118.2	278.1748	3664	9	34.8	293.4732
10	3473	321	174.6	278.1748	4038	15.6	45.6	323.4293
11	3674	337.2	180.6	294.2742	4291	13.2	70.8	343.6936
12	3473	317.4	176.4	278.1748	4199	18.6	35.4	336.3248
13	3766	331.8	204.6	301.643	4289	13.8	74.4	343.5335
14	3480	354.6	160.2	278.7355	4534	44.4	65.4	363.1571
15	4043	349.2	199.2	323.8297	4680	161.4	150	374.8511
16	4230	342	169.8	338.8078	4680	186.6	162.6	374.8511
17	5307	365.4	169.8	425.0716	5827	100.2	186	466.7217
18	5904	359.4	157.2	472.8891	6012	12.6	175.8	481.5396
19	5869	372.6	147.6	470.0858	6189	85.2	164.4	495.7166
20	6466	351.6	145.8	517.9033	6752	77.4	199.2	540.8109
21	6060	351.6	150	485.3842	6597	21	180	528.3959
22	6341	368.4	173.4	507.8913	6623	27	187.8	530.4785
23	6632	412.8	138.6	531.1993	6919	156.6	163.8	554.187
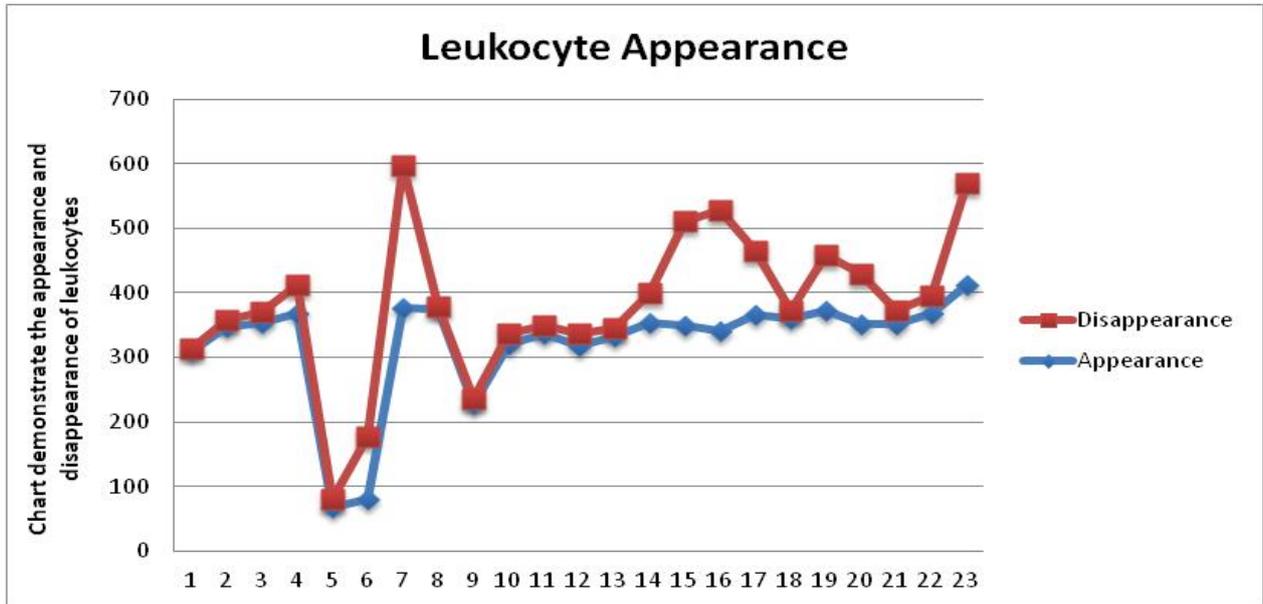
Fig 4: represents a first appearance, red color represent when the leukocytes disappearance.

XIII. LEUKOCYTES POSITION

Now we are determining the specific position of every leukocyte in X-direction and Y-direction. So this step, it's more important to demonstrate the relative leukocyte position, velocity and acceleration of moving leukocytes through an inflamed venule. In Table 6 we presented the positions of every leukocyte in Y-direction and Y-direction.

Table 6: leukocytes position in X-direction, Y-direction and the corresponding time for first leukocyte, as a position of the leukocyte center inside venule units in µm (micrometer)

time	px	py
0.080096	346	170.4
3.283952	377.2	173.4
5.206266	391	179.4
7.368869	412	180.6
8.249929	413.2	180
9.931954	426.4	179.4
11.69407	436.6	186
14.41735	488.2	189.6
16.41976	522.4	187.8
20.0241	565.6	187.2
24.90998	619.6	193.8
31.31769	648.4	206.4
31.95846	650.2	202.2

$$y = -0.0344x^2 + 11.414x + 332.37$$
$$R^2 = 0.9818$$

$$y = 0.1016x^2 + 1.0996x + 171.76$$
$$R^2 = 0.8986$$
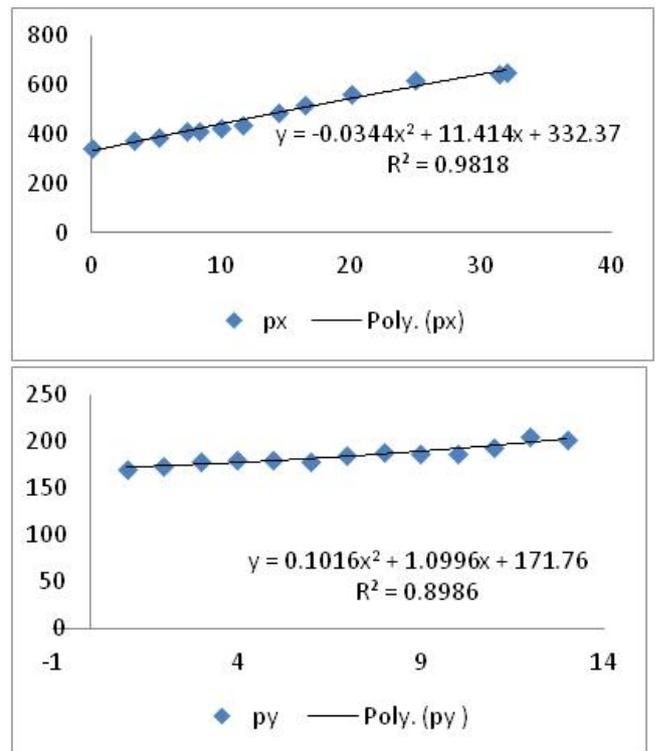
Fig 5: Fig6: Data (points) and fitted (lines) of positions of one leukocyte (L1) in sequential frames.(Px) position of leukocyte in x-direction with time,(Py) position of leukocyte in Y-direction with time.
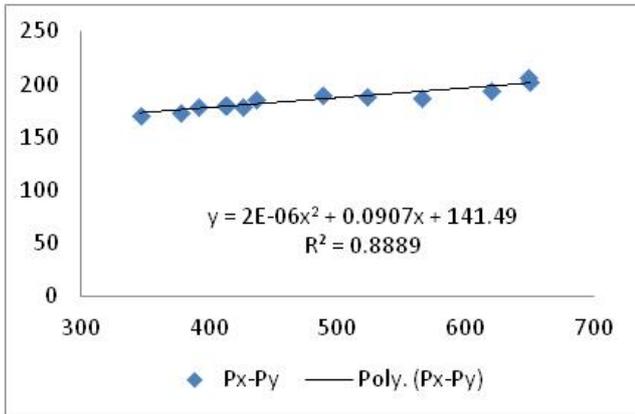
Fig 7:(Px-Py) the leukocyte track.

Force Calculation Using Physically Properties

Leukocyte volumes and Leukocyte density have been determined on isolated leukocyte as following [131]:

Leukocyte density =1.067g/ml

Leukocyte volumes =   468-/+24 cu mu

$\because$ Leukocyte mass =density × volume.

$\therefore$ Leukocyte mass = 473.748 g/ml. cu mu $\rightarrow$ leukocyte

Mass = 73.748$\times 10^{-4}$ =0.0473.748gm

Regarding to equation (15)

$$F = \frac{3}{2}\pi R^3 pg + 6\pi\mu R v_\infty \qquad (15)$$

The first term on the right side of past equation represent the buoyant force and the second result from the blood motion about the leukocyte.it convenient for later discussions to designate these tow term as F_s (equation (16) the force exerted even if the blood is stationary) and F_k (equation (17) the force associated with the blood movement) for the problem at the hand these forces are:

$$F_s = \frac{3}{2}\pi R^3 pg$$

$$F_k = 6\pi\mu R v_\infty$$

From equation (16):

$$F_s = \frac{3}{2}\pi R^3 pg \rightarrow Ma_i = 0.0473.748 \ * a_i \ mu/sec2.$$

Where M represents the mass of leukocyte and represents the acceleration of leukocyte. Therefore the

X-position was fitted   to a 2nd order pronominal the equation of for the X-position was fitted to be:

p_x=0.0344x^2 + 11.414x + 332.37

u_x=0.0688x+11.414.

a_x=0.0688 mu/sec^2

F $_{hydrodynamic}$ =m $_a$HD

=ma$_{x=}$0.0473.748*0.0688=0.00325938624 ps

Py= = 0.1016x^2 + 1.0996x + 171.76

u_y=0.2032x + 1.0996x.

a_y=0.2032 mu/sec^2

F $_r$= ma $_y$ $_=$00.0473.748*0.2032 =0.00962655936 dynes.

Assume a_y=a$_z$=0.00962655936 dynes.

So

$$F_t = \sqrt{F_x^2 + F_y^2 + F_z^2}$$

$$\rightarrow \sqrt{(0.00325938624) + 2(0.00962655936)}$$

= 0.013998746 dynes

XIV.   DISCUSSION AND CONCLUSION

In this paper we have implemented a fuzzy   logic-based procedure for segmenting dynamic clusters of the moving leukocytes frame captured intervital microcopy of a rare venule   of about 28 micrometers in diameter. The main objectives of this study are:

- To develop a new technique by which the performance of the optimal threshold detection would be enhanced.
- To use the fuzzy similarity techniques in the field of biomedical image analyses.
- To calculate the velocity and acceleration of leukocyte.
- To detonate the force acting on the leukocytes.

The result   demonstrated that utilization of the Log-Normal distribution outperformance other tested distributions of similar complexity, also Log-Normal edge detector produced continuous and precise edges, and it was also identified edges accurately. The Log-Normal edge detector performs better than all others detectors due to the ability of Log-normal to deal with asymmetric and sympatric data. Beta edge detector identified surprisingly similarly to the Gamma detector, and both have a major drawback of identifying the edges with spotty and not contiguous.

Tracking of leukocytes was made semi-manual due to the restriction resolution of the image and the lack of the available automated segmentation algorithms, owever the aim of this project was to automate the process of segmentation but not

the tracking process. This would a subject of a future work.It was possible to compute the velocity and acceleration for Instantaneous leukocytes.

The tracks, velocity and acceleration were smoothed using physical properties and gouvring force, electromagnetic force and gravitational forces. From theses we were able to compute the average forces. It was found that the force acting on the leukocyte during its path through small venules is about **0.013998746** dynes.

The error in our calculation was as one pixel to the naked eye and is therefore relative.

From the results the lack of information on the third dimension is clearly noticed when there is no change in time either in the x- or the y-directions. This indicates that the objects probably move in the other direction perpendicular to the imaging device and therefore is undetectable. The fitting of the data shows very complicated leukocyte tracks. This may be attributed to the complex nature of inflammation which involves biochemical reactions of selection and other biomarkers, a process dependent on locality and time. The error in our calculation was as one pixel to the naked eye and is therefore relative.

REFERENCES

[1] M. Zikos, E. Kaldoudi, and S. C. Orphanoudakis. "Medical Image Processing" (1997).

[2] J.C Russ, The image processing handbook. CRC press, 2006.

[3] P M Mather, "Computer processing of remotely-sensed images." (1987): 125.

[4] S.M Kuo and D. Morgan. Active noise control systems: algorithms and DSP implementations. John Wiley & Sons, Inc., 1995.

[5] J.V Hajnal, and L.H Derek. Medical image registration. CRC press, 2010.

[6] J.Schneider, G.Peltri, N.Bitterlich, et al. Fuzzy logic-based tumor marker profiles including a new marker tumor M2-PK improved sensitivity to the detection of progression in lung cancer patients. Anticancer Research. 2003;23(2A):899–906.

[7] B.N Jobse, et al. "Evaluation of allergic lung inflammation by computed tomography in a rat model in vivo." European Respiratory Journal 33.6 (2009): 1437-1447.

[8] S. T. Acton and K. Ley, "Tracking leukocytes from in vivo video microscopy using morphological anisotropic diffusion", Proc. IEEE Int. Conf. Image Proc. 2001, vol. 2, pp.300 -303

[9] J. Tang and S. T. Acton, "Vessel boundary tracking for intravital microscopy via multilevel gradient vector flow snakes", IEEE Trans. Biomed. Eng., vol. 51, pp.316 -324 2004

[10] K.E Normanet , et al. "Sialyl Lewisx (sLex) and an sLexMimetic, CGP69669A, Disrupt E-Selectin–Dependent Leukocyte Rolling In Vivo." Blood 91.2 (1998): 475-483.

[11] U. Jung, K. E Norman, et al. "Transit time of leukocytes rolling through venules controls cytokine-induced inflammatory cell recruitment in vivo." Journal of Clinical Investigation 102.8 (1998): 1526

[12] A.M.Artoli, A.Sequeira, A.S .Silva, and C.Saldanha, Leukocyte rolling and recruitment by endothelial cells: hemorheological experiments and numerical simulations, Journal of Biomechanics, (2007).

[13] R.C. Gonzalez, and R.E. Woods, "Digital image processing," 3rd ed, (Prentice Hall, 2008).

[14] N.Ray.S.Acton and K.Ley. Tracking leukocytes in vivo with shape and size constrained active contours. Medical Imaging, IEEE Transactions on 21, 10 (Oct. 2002), 1222{1235.

[15] N.Ray, and S.Acton. Motion gradient vector ow: an external force for tracking rolling leukocytes with shape and size constrained active contours.Medical Imaging, IEEE Transactions on 23, 12 (Dec. 2004), 1466{1478.

[16] J.Cui, S.T Acton and Z.A Lin. monte carlo approach to rollingleukocyte tracking in vivo. Medical Image Analysis 10, 4 (2006), 598 { 610.Special Issue on Functional Imaging and Modelling of the Heart (FIMH 2005).

[17] D. Mukherjee, N. Ray, and Acton, S. Level set analysis for leukocyte detection and tracking. Image Processing, IEEE Transactions on 13, 4 (April 2004), 562{572.

[18] E.Eden, D.Waisman, et al. An automated method for analysis of ow characteristics of circulat-ing particles from in vivo video microscopy. Medical Imaging, IEEE Transactions on 24, 8 (Aug. 2005), 1011{1024.}

[19] C.ANaranjo,K.E Bremner,M. Bazoon,et al. Using fuzzy logic to predict response to citalopram in alcohol dependence. Clinical Pharmacology and Therapeutics. 1997;62(2):209–224.

[20] A.M ARTOLI, et al. Leukocytes rolling and recruitment by endothelial cells: Hemorheological experiments and numerical simulations. Journal of biomechanics, 2007, 40.15: 3493-3502.

[21] Z.Cai. Fuzzy particle filter used for tracking of leukocytes. In Intelligent Information Technology Application Workshops, 2008. IITAW'08. International Symposium on (pp. 562-565). IEEE.

[22] L.A ZADEH, Fuzzy logic computing with words. Fuzzy Systems, IEEE Transactions on, 1996, 4.2: 103-111.

[23] T. LAW, H. Hidenori,et al. Image filtering, edge detection, and edge tracing using fuzzy reasoning. Pattern Analysis and Machine Intelligence, IEEE Transactions on, 1996, 18.5: 481-491.

[24] F.Russo. Edge detection in noisy images using fuzzy reasoning. In Instrumentation and Measurement Technology Conference, 1998. IMTC/98. Conference Proceedings. IEEE (1998, May ,Vol. 1, pp. 369-372). IEEE.

[25] V.Boskovitz, H. Guterman, An adaptive neuro-fuzzy system for automatic image segmentation and edge detection. Fuzzy Systems, IEEE Transactions on,2002, 10(2), 247-262.

[26] E.E Kerre, and M. Nachtegael. Fuzzy techniques in image processing (Vol. 52). Springer2000.

[27] G.J Klir and B.Yuan. Fuzzy sets and fuzzy logic (pp. 487-499). New Jersey: Prentice Hall,1995.

[28] X. Golay,S. Kollias,G. Stoll, et al. A new correlation based fuzzy logic clustering algorithm for FMRI. Magnetic Resonance in Medicine, 40(2), 249-260.

[29] N.R. Pal and S.K. Pal. A review on image segmentation techniques. Pattern recognition, 26(9), 1277-1294. (1993).

[30] R. B. Bird, Stewart, W. E., & Lightfoot, E. N. (1960). Transport phenomena (Vol. 2). New York: Wiley.